© 2014. Published by The Company of Biologists Ltd | Development (2014) 141, 2848-2854 doi:10.1242/dev.108811

RESEARCH ARTICLE

# mTORC1 signaling controls mammalian skeletal growth through stimulation of protein synthesis

**Jianquan Chen[1] and Fanxin Long[1,2,3,*]**


## ABSTRACT

Much of the mammalian skeleton is derived from a cartilage template that undergoes rapid growth during embryogenesis, but the molecular mechanism of growth regulation is not well understood. Signaling by mammalian target of rapamycin complex 1 (mTORC1) is an evolutionarily conserved mechanism that controls cellular growth. Here we report that mTORC1 signaling is activated during limb cartilage development in the mouse embryo. Disruption of mTORC1 signaling through deletion of either mTOR or the associated protein Raptor greatly diminishes embryonic skeletal growth associated with severe delays in chondrocyte hypertrophy and bone formation. The growth reduction of cartilage is not due to changes in chondrocyte proliferation or survival, but is caused by a reduction in cell size and in the amount of cartilage matrix. Metabolic labeling reveals a notable deficit in the rate of protein synthesis in Raptor-deficient chondrocytes. Thus, mTORC1 signaling controls limb skeletal growth through stimulation of protein synthesis in chondrocytes.


**KEY WORDS: mTOR, mTORC1, Raptor, Rptor, Cartilage, Chondrocyte, Mouse**

## INTRODUCTION

The limb skeleton of mammals is derived from cartilage templates through endochondral ossification (Kronenberg, 2003; Long and Ornitz, 2013). The process begins with condensation of mesenchymal cells within the embryonic limb bud. Subsequently, cells at the core of mesenchymal condensation differentiate into chondrocytes, whereas those at the periphery give rise to the perichondrium. Following the initial proliferation that produces an elongated cartilage template, chondrocytes become increasingly organized into morphologically distinct domains. At either end of the template the proliferating chondrocytes exhibit a rounded morphology (round chondrocytes), but become flattened and stacked in columns (columnar chondrocytes) towards the middle of the cartilage rod. The columnar chondrocytes produce a large amount of extracellular matrix and also proliferate at a higher rate than the round cells (Long et al., 2001). Further towards the center of the template, the columnar chondrocytes eventually stop proliferating and enter the hypertrophic stage. A recent study indicates that chondrocyte hypertrophy can be further divided into three progressive stages of volume enlargement based on changes in the density of cellular dry mass (Cooper et al., 2013). During the first phase, cells increase both dry mass and fluid volume, thus maintaining the same density of dry mass as the prehypertrophic cells; this is then followed by a swelling phase that reduces the dry mass density, and the final phase when both dry mass and fluid volume increase again without changing the dry mass density. Concurrent with chondrocyte hypertrophy, cells within the perichondrium surrounding the hypertrophic zone differentiate into osteoblasts that produce a nascent bone collar. The hypertrophic chondrocytes are generally believed to undergo apoptosis, followed by invasion of blood vessels from the perichondrium. The invading vasculature not only triggers resorption of the hypertrophic cartilage matrix and formation of the bone marrow cavity, but also brings in osteoblast precursors that eventually produce cancellous bone within the marrow cavity (Maes et al., 2010). Overall, proper regulation of chondrocyte progression through proliferation and hypertrophy is crucial for skeletal growth, but relatively little is known about the intracellular signaling mechanisms responsible for these transitions.

Mammalian (or mechanistic) target of rapamycin (mTOR) is an evolutionarily conserved serine/threonine kinase that integrates various inputs from growth factors and nutrients to regulate cell growth, proliferation and survival (Sengupta et al., 2010b). mTOR functions as the catalytic subunit in two functionally distinct signaling complexes: mTOR complex 1 (mTORC1) and complex 2 (mTORC2) (Sengupta et al., 2010b; Thoreen et al., 2009). The complexes are distinct by virtue of specific components, such as Raptor (also known as Rptor) for mTORC1 and Rictor for mTORC2, and by their different downstream effectors (Jacinto et al., 2004; Sarbassov et al., 2004). mTORC1 is best known for phosphorylating p70 S6 kinase (p70S6K; also known as RPS6KB1) and eukaryotic translation initiation factor 4E binding protein 1 (4EBP1; also known as EIF4EBP1) to regulate protein synthesis (Thoreen et al., 2012). Global deletion of mTOR or Raptor in the mouse leads to early postimplantation lethality (Gangloff et al., 2004; Guertin et al., 2006; Murakami et al., 2004). Subsequent tissue-specific knockout studies have identified crucial roles for mTORC1 in several tissues, but its function in skeletal development has not been examined genetically (Bentzinger et al., 2008; Polak et al., 2008; Yilmaz et al., 2012).

Here, through deletion of either mTOR or Raptor, we demonstrate that mTORC1 signaling is required for optimal protein production in chondrocytes, thus controlling cell size, the amount of cartilage matrix and, ultimately, skeletal size. This study therefore identifies mTORC1 as a crucial regulator of skeletal growth during embryogenesis.

## RESULTS

### mTORC1 signaling during endochondral bone development

To gain insight into mTOR signaling in the developing long bone, we performed immunofluorescence staining for phosphorylation of ribosomal protein S6 (P-S6) by p70S6K at residues S240 and S244, an established readout for mTORC1 signaling, on sections of mouse embryonic limbs (Sengupta et al., 2010a). We first examined the humerus at embryonic day (E) 15, before the marrow cavity was formed. Here, P-S6 was detected at a relatively low level in a 'salt and pepper' pattern among the round chondrocytes (Fig. 1A,B, yellow

[1]Department of Orthopaedic Surgery, Washington University School of Medicine, St Louis, MO 63110, USA. [2]Department of Medicine, Washington University School of Medicine, St Louis, MO 63110, USA. [3]Department of Developmental Biology, Washington University School of Medicine, St Louis, MO 63110, USA.

*Author for correspondence (longf@wudosis.wustl.edu)

**Received 6 February 2014; Accepted 13 May 2014**

Development (2014) 141, 2848-2854 doi:10.1242/dev.108811

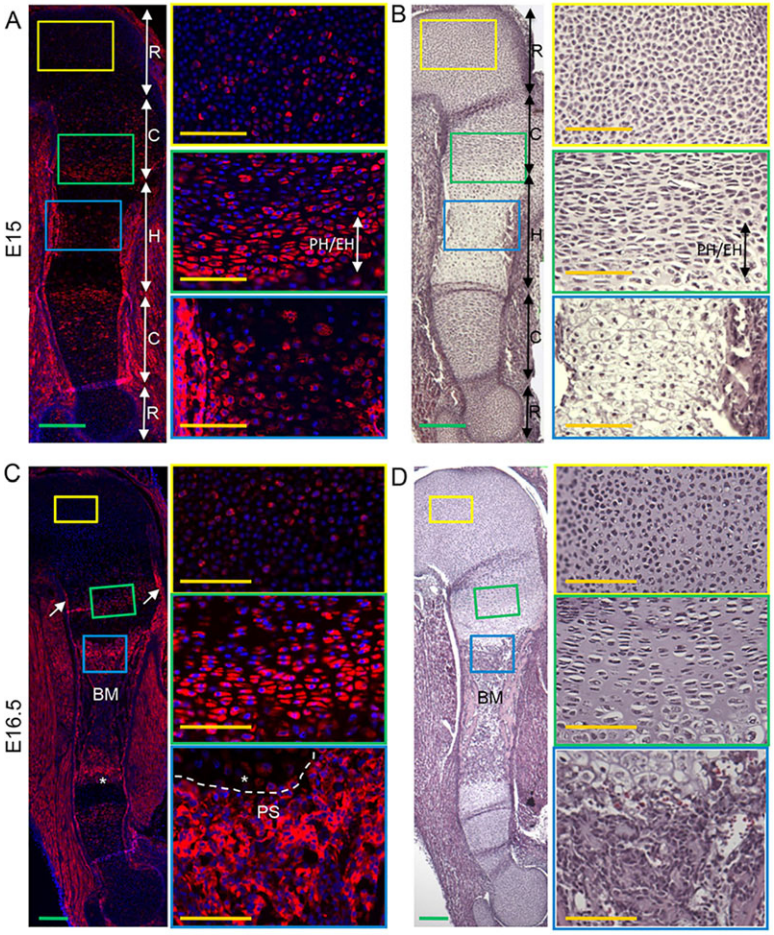


**Fig. 1. mTORC1 signaling during endochondral bone development.** Phosphorylated S6 (P-S6) immunofluorescence (A, C) or H&E staining (B,D) on longitudinal sections of mouse humerus at E15 (A,B) or E16.5 (C,D). Boxed areas are shown at higher magnification to the right. Dashed line in C indicates the boundary between hypertrophic cartilage and primary spongiosa; P-S6 signal in red; DAPI staining of DNA in blue. R, round chondrocytes; C, columnar chondrocytes; PH/EH, prehypertrophic/early hypertrophic chondrocytes; BM, bone marrow cavity; PS, primary spongiosa. Arrows indicate perichondrium; asterisks indicate terminal hypertrophic chondrocytes. Scale bars: green, 2 mm; orange, 1 mm.

boxes). The staining was notably increased in both intensity and uniformity within the columnar region, with the prehypertrophic and early hypertrophic chondrocytes exhibiting the most prominent, nearly homogeneous signal (Fig. 1A,B, green boxes). The P-S6 signal declined rapidly beyond the early hypertrophic stage, resulting in little staining within much of the hypertrophic region (Fig. 1A,B). P-S6 was somewhat reactivated in cells at the final stage of hypertrophy (Fig. 1A,B, blue boxes). At E16.5, the staining pattern of P-S6 within the different zones of cartilage was identical to that at E15 (Fig. 1C,D). However, at this stage, the central hypertrophic region was replaced by a nascent marrow cavity, and the terminal hypertrophic chondrocytes were found near the chondro-osseous junction. These cells, like those at E15, also exhibited some reactivation of P-S6 (Fig. 1C, asterisk). Besides chondrocytes, the osteoblast precursors within either the perichondrium or the primary spongiosa also exhibited a robust P-S6 signal (Fig. 1C, arrows, PS in blue box). Because deletion of Raptor abolished the P-S6 signal in chondrocytes and osteoblast precursors, we conclude that P-S6 faithfully reflects mTORC1 signaling in the developing skeleton (supplementary material Fig. S2B). Overall, the dynamic pattern of mTORC1 signaling indicates that the pathway is likely to play a role in normal skeletal development.

### mTORC1 is crucial for embryonic skeletal growth

To examine directly the role of mTOR in skeletal development, we deleted the gene with Prx1-Cre, which targets mainly the limb, the cranial and the interlimb flank mesenchyme (Logan et al., 2002). Briefly, *Prx1-Cre; Mtor*$^{f/+}$ male mice were mated with *Mtor*$^{f/f}$ females to produce *Prx1-Cre; Mtor*$^{f/f}$ embryos (hereafter mTORCKO). The mutant mice were born alive but died shortly after birth; their limbs were severely diminished, and ~50% also exhibited exencephaly (supplementary material Fig. S1A,B). Whole-mount skeletal staining at E18.5 revealed a clear deficiency in ossification of the skull and the sternum, in addition to the marked shortening of appendicular bones (supplementary material Fig. S1C-H). The limb skeleton was correctly patterned but each element was greatly reduced in size (Fig. 2A-D). Direct measurements of the humerus indicated that the total length and the relative bone-collar length (normalized to total length) were decreased to 34.2% and 70.6% of normal values, respectively (Fig. 2E). Histological analyses of the ulna revealed that, in contrast to the well-established marrow cavity that is normally present at E18.5, the mutant element maintained a cartilaginous core (supplementary material Fig. S1I,J). Similar defects were observed with the other limb bones of mTORCKO mice. Thus, loss of mTOR severely impairs skeletal growth.

Because mTOR can function through either mTORC1 or mTORC2, we next assessed the specific contribution of mTORC1. For this, we deleted the gene encoding the mTORC1-specific Raptor with Prx1-Cre in the same way as for mTOR removal. Western blot analyses of limb bud protein extracts confirmed that Raptor and P-S6 were markedly reduced in *Prx1-Cre; Raptor*$^{f/f}$ embryos (hereafter RapCKO) at E12.5 (supplementary material Fig. S2A). The residual signal of Raptor and P-S6 in RapCKO could be due to the ectoderm that Prx1-Cre did not target, or to incomplete deletion in the mesenchyme at this early stage. Regardless, when examined by immunostaining at E16.5, the P-S6 signal was undetectable from the cartilage and the perichondrium (supplementary material Fig. S2B). Importantly, the RapCKO embryos exhibited a perinatal phenotype strikingly similar to that of mTORCKO, including very short limbs,

Development (2014) 141, 2848-2854 doi:10.1242/dev.108811

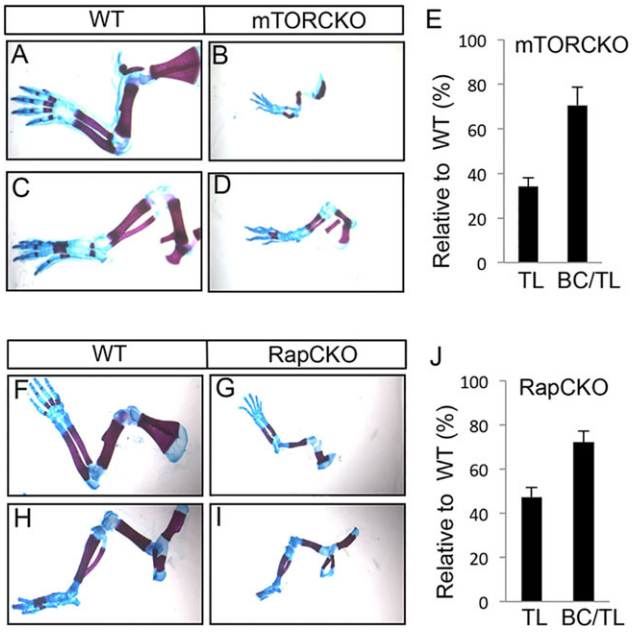


**Fig. 2. mTORC1 is crucial for embryonic skeletal growth.**
(A-D) Representative images of forelimb (A,B) and hindlimb (C,D) skeletons from E18.5 wild-type (WT; A,C) versus mTORCKO (B,D) littermates. (E) Quantification of humerus length in E18.5 mTORCKO relative to WT littermates. (F-I) Forelimb (F,G) and hindlimb (H,I) skeletons from E18.5 WT (F,H) versus RapCKO (G,I) littermates. (J) Quantification of humerus length in E18.5 RapCKO relative to WT littermates. Cartilage is stained blue; bone collar is stained red. TL, total humerus length; BC/TL, ratio of bone collar over total length. *n*=3 for each genotype; error bars indicate s.d.

exencephaly and neonatal death (supplementary material Fig. S2C,D). Whole-mount skeletal staining at E18.5 confirmed the shortening of limb elements as well as ossification defects in the skull and sternum of RapCKO mice, reminiscent of those in mTORCKO (supplementary material Fig. S2E-J). All skeletal elements in the limbs of RapCKO were correctly patterned but greatly reduced in size (Fig. 2F-I). The severity of the size reduction was generally similar in RapCKO and mTORCKO, with the exception of the radius and ulna, which appeared to be more severely affected in the latter genotype (Fig. 2B,G). Measurements of the humerus in RapCKO showed that the total length and the relative bone-collar length were shortened to 47.3% and 72.1% of normal values, respectively. Thus, mTOR appears to drive skeletal growth mainly through mTORC1 signaling.

### mTORC1 enhances chondrocyte growth and matrix production through stimulation of protein translation

To gain insight into how mTORC1 signaling affects skeletal growth, we analyzed the RapCKO embryos further. The reduced skeletal size could be due to impaired cell proliferation. However, BrdU labeling assays at E15.5 did not detect any defect in the proliferation of round or columnar chondrocytes in the RapCKO embryo (Fig. 3A,B). To examine a potential contribution from apoptosis, we performed TUNEL assays in the humerus at several embryonic stages. No apoptosis was detected in proliferative chondrocytes of control or RapCKO embryos at any stage. In the control, apoptotic cells first appeared within the perichondrium flanking the hypertrophic region at E14.5, and then among the terminal hypertrophic chondrocytes at E15.5 (Fig. 3C,E). After the formation of a bone marrow cavity in the control at E16.5 and E18.5, apoptosis was detected at both the periosteum and the chondro-osseous junctions (Fig. 3G,I). In the RapCKO embryo, apoptosis in the perichondrium and hypertrophic chondrocytes did not occur until E16.5 (Fig. 3D,F,H). Moreover, at E18.5 the apoptotic hypertrophic chondrocytes in RapCKO remained at the center of the humerus instead of being replaced by a marrow cavity (Fig. 3J). Thus, disruption of mTORC1 signaling at the mesenchymal progenitor stage did not cause ectopic apoptosis of chondrocytes, but instead delayed the onset of normal apoptosis and impaired the removal of apoptotic hypertrophic chondrocytes. Whether these defects reflect direct regulation by mTORC1 or are secondary consequences of some earlier effects is not known at present. Nonetheless, the impact of mTORC1 on skeletal growth cannot be explained by changes in chondrocyte proliferation or survival.

Chondrocyte hypertrophy is a major driving force for limb skeletal growth. We therefore examined the status of hypertrophy in the RapCKO embryo. Histological sections revealed a much shorter hypertrophic zone in the humerus of RapCKO embryos at both E14.5 and E15.5, and this shortening was disproportionate to the reduction in total length (Fig. 4A,B; supplementary material Fig. S3A,B). *In situ* hybridization detected expression of the hypertrophic chondrocyte marker *Col10a1* in the humerus of E13.5 wild-type but not RapCKO littermate embryos (supplementary material Fig. S3C,D). Thus, lack of mTORC1 delayed the onset of chondrocyte hypertrophy. As expected from the delay in hypertrophy, bone collar formation was also impeded in the RapCKO embryo. Whereas a bone collar stained positive by the von Kossa method is normally evident at E14.5, it was not detectable in the RapCKO embryo until E16.5 (Fig. 4C). As shown above, at E18.5 the central hypertrophic cartilage persisted in the mutant humerus, instead of being replaced by a marrow cavity (Fig. 4D). *In situ* hybridization showed that the central hypertrophic chondrocytes in the mutant sample no longer expressed *Col10a1* but activated *Mmp13*, indicating their status of terminal hypertrophy (Fig. 4D). The terminal status of the cells was also supported by the observation above that some were undergoing apoptosis (Fig. 3I). However, a closer examination revealed that these cells were considerably smaller than their normal counterparts (Fig. 4E,F). The reduced size of RapCKO hypertrophic chondrocytes was unlikely to be due to the absence of a primary ossification center in the mutant bones because, even when compared with E15 wild-type embryos that had not yet developed the ossification center, the E18.5 RapCKO mice still had significantly smaller hypertrophic chondrocytes (Fig. 4F). Thus, in the absence of mTORC1 signaling, hypertrophic chondrocytes failed to attain a normal size. Taken together, the results so far demonstrate that mTORC1 controls not only the initiation of hypertrophy, but also the ultimate size and the eventual removal of the hypertrophic chondrocytes.

Besides hypertrophy, the size of other chondrocytes and the amount of cartilage matrix also contribute to the size of skeletal elements. Therefore, we examined the round and columnar regions by histomorphometry. Indeed, both areas exhibited a higher cell density in the humerus of E18.5 RapCKO than in the littermate control (Fig. 5A-C). Further quantification of the columnar region identified a clear decrease in both cell size and matrix area per cell (Fig. 5D,E). Analyses of the humerus at E13.5 provided similar results (supplementary material Fig. S4). Thus, loss of mTORC1 reduces both the size of chondrocytes and the amount of extracellular matrix that they produce.

These findings prompted us to determine whether mTORC1 normally stimulates protein translation in chondrocytes. We performed metabolic labeling experiments with primary cultures of chondrocytes with Raptor either intact or deleted *in vitro* with an adenovirus expressing Cre. Western blot analyses confirmed

Development (2014) 141, 2848-2854 doi:10.1242/dev.108811

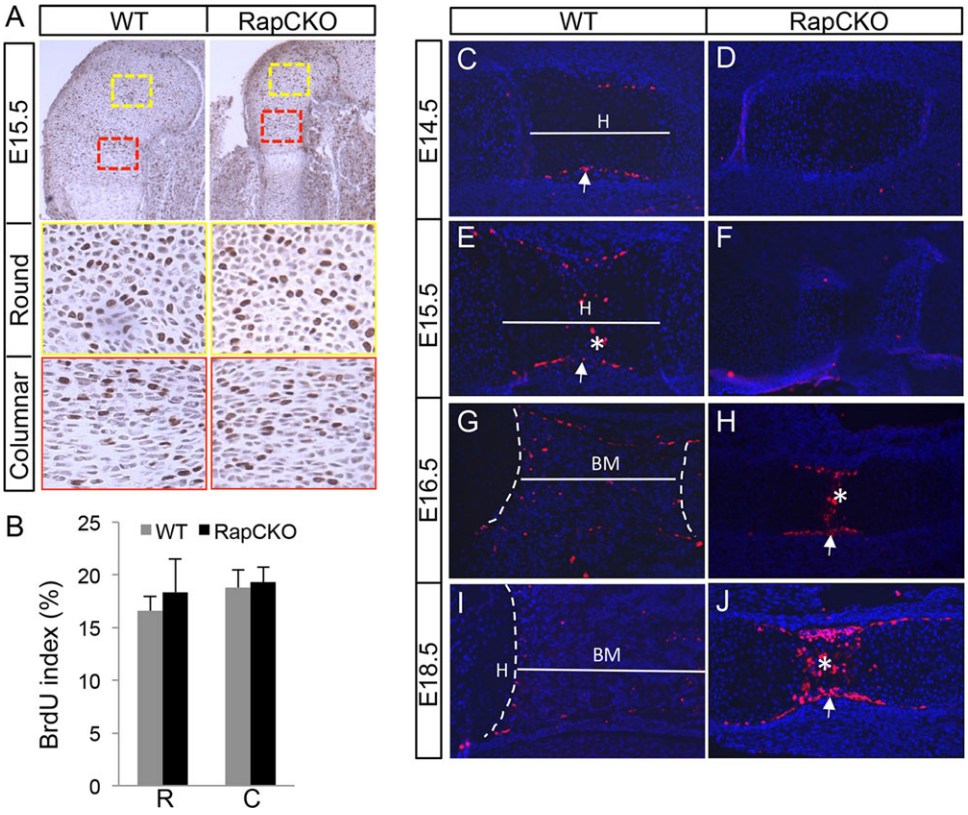


**Fig. 3. mTORC1 does not have a major impact on chondrocyte proliferation or survival.** (A) BrdU labeling of chondrocytes in the humerus of E15.5 WT versus RapCKO littermates. Boxed areas from round chondrocyte and columnar chondrocyte regions are shown at a higher magnification beneath. (B) Quantification of BrdU labeling in chondrocytes. *n*=3 embryos for each genotype; error bars indicate s.d. R, round chondrocytes; C, columnar chondrocytes. (C-J) TUNEL assays of longitudinal humeral sections from E15.5-18.5 WT (C,E,G,I) versus RapCKO (D,F,H,J) littermates. H, hypertrophic chondrocytes; BM, bone marrow cavity. Arrows point to apoptotic cells in the perichondrium; asterisks indicate terminal hypertrophic chondrocytes undergoing apoptosis.

effective Cre-mediated deletion of Raptor and the expected decrease in the phosphorylation of 4EBP1 and S6 (Fig. 6A). By contrast, phosphorylation of AKT (at S473), a known target of mTORC2, was not impaired but rather increased upon mTORC1 disruption, a phenomenon previously reported in other systems (Fig. 6A) (Laplante and Sabatini, 2012). Importantly, the Raptor-deficient chondrocytes exhibited a marked deficiency in protein synthesis compared with the control cells (Fig. 6B).

Overall, this study establishes mTORC1 as a crucial determinant of chondrocyte size and matrix production during endochondral skeletal development through its stimulation of protein translation.

## DISCUSSION

We have identified mTORC1 as a crucial regulator of embryonic skeletal growth in mice. Our data indicate that physiological mTORC1 signaling increases the cell size and the amount of extracellular matrix proteins produced by chondrocytes at all stages of maturation. In addition, normal mTORC1 activity is necessary for the timely transition of chondrocytes to hypertrophy, as well as for the final removal of hypertrophic chondrocytes. The direct impact of mTORC1 on the overall rate of protein translation in chondrocytes is likely to be central to the function of this protein complex in skeletal growth.

Chondrocyte hypertrophy is a principal driving force in skeletal growth. Recent studies have identified three distinct phases of volume increase during hypertrophy. Both the first and third phase involve increases in dry mass production, whereas the second phase of expansion is due to fluid accumulation in the cell (Cooper et al., 2013). Interestingly, our data show that mTORC1 signaling is robustly activated in the prehypertrophic/early hypertrophic stage, but then becomes undetectable until being reactivated in the final phase of hypertrophy. Therefore, mTORC1 signaling might drive the increase in dry cell mass in the first and third phases of hypertrophy, therefore contributing to the final size of hypertrophic chondrocytes. The final stage of chondrocyte hypertrophy is normally followed by apoptosis and replacement by a marrow cavity formed through blood vessel invasion. Previous work in bat and mouse limbs has indicated that the entire hypertrophic zone in a growth plate is normally turned over within ~24 h (Cooper et al., 2013; Farnum et al., 2008). Here we show that, without mTORC1, the hypertrophic chondrocytes failed to turn over even though they transitioned to the final stages of expressing MMP13 and undergoing apoptosis. This observation raises the intriguing possibility that mTORC1 activity in the terminal hypertrophic chondrocytes might be intrinsically necessary for blood vessel invasion and for the removal of hypertrophic cartilage, but we cannot exclude the possibility that the defect might be secondary to the loss of mTORC1 in other cell types in the limb.

It should be noted that because mTOR or Raptor was deleted by Prx1-Cre at the mesenchymal progenitor stage in our study, potential defects in the progenitors might have contributed to the dramatic size reduction in the limb skeleton. Indeed, we have observed smaller cartilage primordia in the limbs of E11.75 RapCKO embryos when compared with littermate controls. Thus, mTORC1 signaling appears to stimulate embryonic skeletal growth by regulating both the initial formation and the subsequent growth of the cartilage template. Future experiments with more stage-specific approaches (e.g. Col2-Cre) will be necessary to distinguish the relative contribution of each stage to overall skeletal growth.

It is worth noting that mTORC1 activity markedly decreases following the onset of hypertrophy. A recent study showed that hyperactivation of mTORC1 via the deletion of *Lkb1* caused overgrowth of the columnar region, highlighting the importance of mTORC1 suppression for the transition of the cells to hypertrophy (Lai et al., 2013). It is not yet clear at present whether *Lkb1*

Development (2014) 141, 2848-2854 doi:10.1242/dev.108811

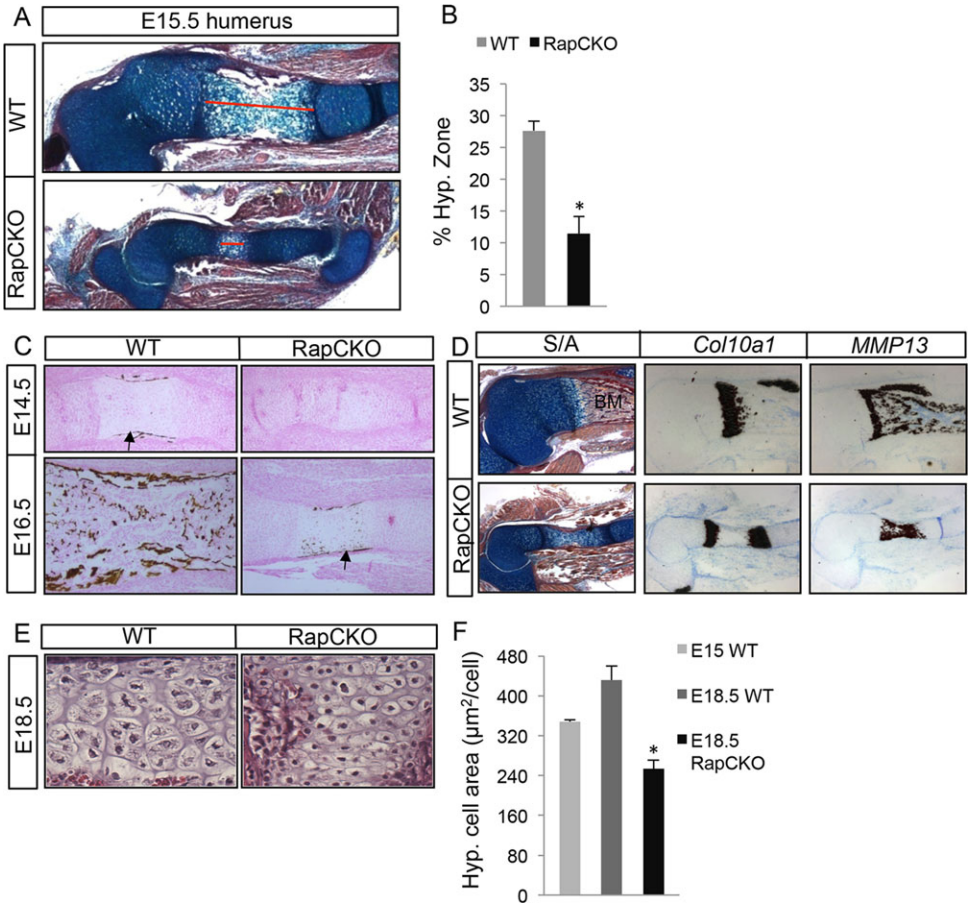


**Fig. 4. mTORC1 controls multiple aspects of chondrocyte hypertrophy.** (A) Alcian Blue/Picrosirius Red staining of longitudinal humeral sections from E15.5 WT and RapCKO littermates. Red line indicates the length of the hypertrophic zone. (B) Length of the hypertrophic zone relative to total humerus length. (C) Von Kossa staining of longitudinal humerus sections from E14.5 or E16.5 WT versus RapCKO littermates. Arrows indicate nascent bone collar. (D) Alcian Blue/Picrosirius Red (S/A) staining and *in situ* hybridization analyses (dark red) on adjacent humeral sections from E18.5 WT and RapCKO littermates. BM, bone marrow cavity. (E) Histology of the hypertrophic zone in the humerus of E18.5 WT versus RapCKO littermates. (F) Average size of hypertrophic chondrocytes on sections. (B,F) *$P$<0.05, $n$=3 animals per genotype; error bars indicate s.d.

activation represents a normal regulatory step during the progression of chondrocyte hypertrophy.

Similarly, it is unclear which extracellular signals are responsible for the dynamic regulation of mTORC1 activity at the various stages of chondrocyte maturation. Insulin-like growth factor (IGF) signaling is likely to play a role because it is known to activate mTORC1 in a variety of tissues, and IGF2 together with the signaling receptor IGF1R are expressed in the growth plate chondrocytes (Oldham and Hafen, 2003; Wang et al., 1995). Disruption of IGF1, IGF2 or IGF1R reduces overall skeletal growth (Baker et al., 1993; Liu et al., 1993; Long et al., 2006). In particular, deletion of *Igf1* resulted in a reduced final size of hypertrophic chondrocytes, apparently due to failure in the third-phase expansion (Cooper et al., 2013; Lupu et al., 2001; Wang et al., 1999). Thus, IGF signaling is likely to contribute to mTORC1 activity in chondrocytes. However, because the skeletal defect caused by mTORC1 deletion is more severe than that in the *Igf1r* knockout embryo (Liu et al., 2013), other signals must also contribute to mTORC1 activation to ensure proper skeletal growth.

## MATERIALS AND METHODS

### Mouse strains

*Prx1-Cre*, *Mtor*$^{f/f}$ and *Raptor*$^{f/f}$ mouse lines are as previously described and were purchased from the Jackson Laboratory (Logan et al., 2002; Risson et al., 2009; Sengupta et al., 2010a). The Animal Studies Committee at Washington University approved all mouse experimental procedures.

### Analyses of mouse embryos

Whole-mount embryonic skeleton was prepared and stained with Alizarin Red/Alcian Blue essentially as described previously (McLeod, 1980). For analyses on sections, embryonic limbs were dissected out in PBS, fixed in 10% formalin overnight at room temperature, and then processed for paraffin embedding prior to sectioning (6 μm). For detection of mineralization, sections were stained with 1% silver nitrate (von Kossa method) and counterstained with Nuclear Fast Red. For other histology-based analyses on E16.5 or older embryos, limbs were decalcified in 14% EDTA for 24 h after fixation and prior to processing. Hematoxylin and Eosin (H&E) staining and Alcian Blue/Picrosirius Red staining were performed on paraffin sections following standard protocols. *In situ* hybridization was performed with $^{35}$S-labeled riboprobes as previously described (Hu et al., 2005; Joeng and Long, 2009; Long et al., 2004; Long et al., 2001).

### BrdU and TUNEL staining

Pregnant females were injected with BrdU at 0.1 mg/g body weight 2 h before harvest. Embryonic limbs were collected, decalcified, processed and sectioned in paraffin. BrdU detection was performed with a BrdU staining kit (Zymed Laboratories). For quantification of BrdU labeling, sections from at least three animals of each genotype were scored for the percentage of BrdU-positive cells. TUNEL assay was performed with the In Situ Cell Death Detection Kit TMR Red (Roche).

### Western blot and immunofluorescence

For western blot analyses, total proteins were isolated from mouse forelimb buds using RIPA buffer [20 mM Tris (pH 8.0), 150 mM NaCl, 0.1% SDS, 1% NP-40, 0.5% sodium deoxycholate]. Protein samples (30 μg) were separated on 10% SDS-polyacrylamide gels and subjected to a standard western procedure. Antibodies for S6 (Cell Signaling, catalog number 2215), P-S6 (S240/244; Cell Signaling, catalog number 2217), AKT (Cell Signaling, catalog number 9272), P-AKT (S473; Cell Signaling, catalog number 9271), 4EBP1 (Cell Signaling, catalog number 9452), P-4EBP1 (S65; Cell Signaling, catalog number 9451), Raptor (Cell Signaling, catalog

Development (2014) 141, 2848-2854 doi:10.1242/dev.108811

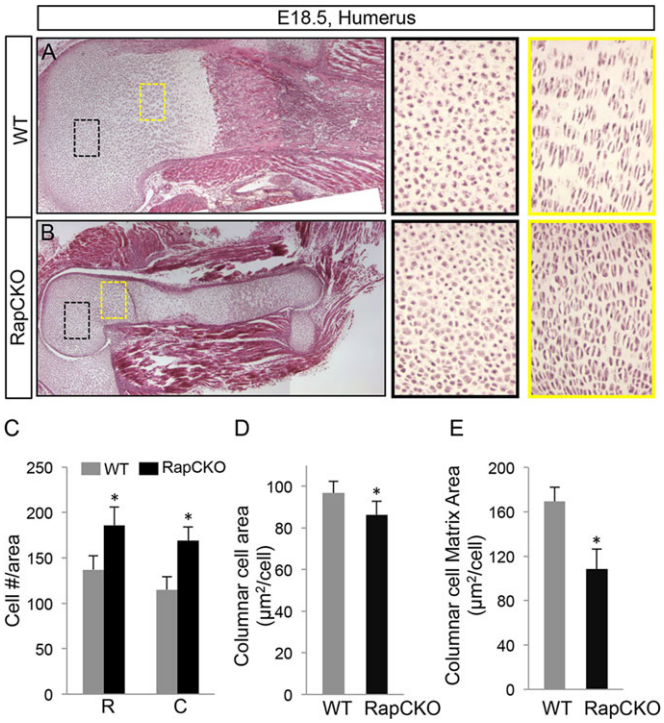


**Fig. 5. mTORC1 regulates chondrocyte size and matrix production.** (A,B) H&E staining of longitudinal humeral sections from E18.5 WT (A) versus RapCKO (B) littermates. Boxed regions are shown at higher magnification to the right. (C) Cell density in round (R) and columnar (C) chondrocyte zones. (D) Average size of columnar chondrocytes on sections. (E) Average matrix area per cell in columnar region. (C-E) *$P$<0.05, $n$=3 mice per genotype; error bars indicate s.d.

number 2280), Rictor (Cell Signaling, catalog number 2140) and β-actin (Cell Signaling, catalog number 4970) were all purchased from Cell Signaling Technology. All antibodies were used at 1:1000 dilution.

For P-S6 immunostaining, paraffin sections of embryonic limbs were deparaffinized, immersed in boiling 10 mM sodium citrate buffer (pH 6.0) for 20 min, and blocked with 5% goat serum before incubation with primary antibody overnight. The sections were then washed three times in PBS, and incubated for 1 h at room temperature with Alexa Fluor 594-conjugated goat anti-rabbit IgG secondary antibody (diluted 1:250 in PBS; Life Technologies, catalog code A-11012). Stained sections were mounted with VECTASHIELD mounting medium containing DAPI (Vector Laboratories).

### Metabolic labeling of protein synthesis

To isolate chondrocytes, the cartilage portion of the rib cage and sternum was dissected from newborn *Raptor*$^{f/f}$ pups, washed with PBS, and then digested with 1.2 mg/ml protease (Sigma) dissolved in PBS at 37°C for 30 min. This was followed by incubation with 3 mg/ml collagenase (Sigma) in DMEM for 60 min at 37°C. The soft tissues were then carefully removed. The remaining rib cage and sternum were further digested in 1.5 mg/ml collagenase in DMEM at 37°C for 4 h. The dissociated chondrocytes were then filtered through a 70 μm cell strainer. Cells were seeded in 6-well plates at $1\times10^6$ cells/well. After overnight culture, cells were infected with adenovirus expressing either green fluorescence protein (Ad-GFP) or Cre (Ad-CRE) at a multiplicity of infection of 100. At 72 h after adenoviral infection, chondrocytes were either lysed with RIPA buffer to evaluate gene deletion efficiency or used for metabolic labeling.

Metabolic labeling was performed as previously described (Thoreen et al., 2012). Briefly, cells were washed once with PBS, then incubated for 30 min in 2 ml cysteine/methionine-free DMEM containing 10% dialysed and heat-inactivated fetal calf serum and 165 μCi EasyTag EXPRESS $^{35}$S protein labeling mix (PerkinElmer, catalog code NEG772002MC). Cells were then lysed with 100 μl RIPA buffer containing protease and

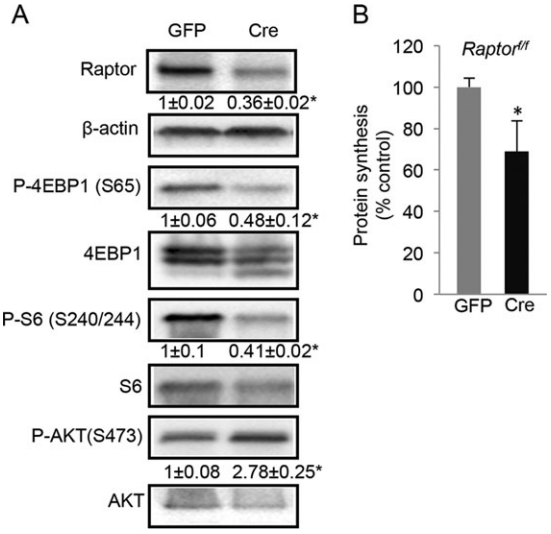


**Fig. 6. mTORC1 regulates protein synthesis in chondrocytes.** (A) Western blot analyses of primary chondrocytes isolated from *Raptor*$^{f/f}$ mice and infected with adenovirus expressing GFP or Cre. Raptor was normalized to β-actin, and phospho-proteins were normalized to the respective total proteins. Ratios in control cells (GFP) were designated 1. Averages and s.d. from three independent experiments are presented. (B) Metabolic labeling in primary chondrocytes as in A. *$P$<0.05, $n$=3; error bars indicate s.d.

phosphatase inhibitors, and soluble protein lysates were isolated by centrifugation. Lysates (10 μl) were then deposited on Whatman filter paper strips; protein was precipitated with 5% trichloroacetic acid (TCA), and washed consecutively with 10% TCA, ice-cold 100% ethanol, and ice-cold acetone. The filter strips were then air-dried at room temperature for 10 min. The amount of $^{35}$S incorporated into protein was quantified using a Beckman LS6500 scintillation counter and normalized to total cell number.

### Statistics

All quantitative data are presented as mean±s.d. from a minimum of three independent samples. $P$<0.05 (two-tailed Student's $t$-test) is considered statistically significant.

#### Competing interests

The authors declare no competing financial interests.

#### Author contributions

J.C. and F.L. conceived the project; J.C. conducted experiments; J.C. and F.L. analyzed data and wrote the paper.

#### Funding

This work is supported by National Institutes of Health grants [R01 DK065789 and R01 AR055923] to F.L. Deposited in PMC for release after 12 months.

#### Supplementary material

Supplementary material available online at
http://dev.biologists.org/lookup/suppl/doi:10.1242/dev.108811/-/DC1

#### References

**Baker, J., Liu, J. P., Robertson, E. J. and Efstratiadis, A.** (1993). Role of insulin-like growth factors in embryonic and postnatal growth. *Cell* **75**, 73-82.

**Bentzinger, C. F., Romanino, K., Cloëtta, D., Lin, S., Mascarenhas, J. B., Oliveri, F., Xia, J., Casanova, E., Costa, C. F., Brink, M. et al.** (2008). Skeletal muscle-specific ablation of raptor, but not of rictor, causes metabolic changes and results in muscle dystrophy. *Cell Metab.* **8**, 411-424.

**Cooper, K. L., Oh, S., Sung, Y., Dasari, R. R., Kirschner, M. W. and Tabin, C. J.** (2013). Multiple phases of chondrocyte enlargement underlie differences in skeletal proportions. *Nature* **495**, 375-378.

**Farnum, C. E., Tinsley, M. and Hermanson, J. W.** (2008). Forelimb versus hindlimb skeletal development in the big brown bat, *Eptesicus fuscus*: functional divergence is reflected in chondrocytic performance in Autopodial growth plates. *Cells Tissues Organs* **187**, 35-47.

Development (2014) 141, 2848-2854 doi:10.1242/dev.108811

**Gangloff, Y.-G., Mueller, M., Dann, S. G., Svoboda, P., Sticker, M., Spetz, J.-F., Um, S. H., Brown, E. J., Cereghini, S., Thomas, G. et al.** (2004). Disruption of the mouse mTOR gene leads to early postimplantation lethality and prohibits embryonic stem cell development. *Mol. Cell. Biol.* **24**, 9508-9516.

**Guertin, D. A., Stevens, D. M., Thoreen, C. C., Burds, A. A., Kalaany, N. Y., Moffat, J., Brown, M., Fitzgerald, K. J. and Sabatini, D. M.** (2006). Ablation in mice of the mTORC components raptor, rictor, or mLST8 reveals that mTORC2 is required for signaling to Akt-FOXO and PKCalpha, but not S6K1. *Dev. Cell* **11**, 859-871.

**Hu, H., Hilton, M. J., Tu, X., Yu, K., Ornitz, D. M. and Long, F.** (2005). Sequential roles of Hedgehog and Wnt signaling in osteoblast development. *Development* **132**, 49-60.

**Jacinto, E., Loewith, R., Schmidt, A., Lin, S., Rüegg, M. A., Hall, A. and Hall, M. N.** (2004). Mammalian TOR complex 2 controls the actin cytoskeleton and is rapamycin insensitive. *Nat. Cell Biol.* **6**, 1122-1128.

**Joeng, K. S. and Long, F.** (2009). The Gli2 transcriptional activator is a crucial effector for Ihh signaling in osteoblast development and cartilage vascularization. *Development* **136**, 4177-4185.

**Kronenberg, H. M.** (2003). Developmental regulation of the growth plate. *Nature* **423**, 332-336.

**Lai, L. P., Lilley, B. N., Sanes, J. R. and McMahon, A. P.** (2013). Lkb1/Stk11 regulation of mTOR signaling controls the transition of chondrocyte fates and suppresses skeletal tumor formation. *Proc. Natl. Acad. Sci. U.S.A.* **110**, 19450-19455.

**Laplante, M. and Sabatini, D. M.** (2012). mTOR signaling in growth control and disease. *Cell* **149**, 274-293.

**Liu, J. P., Baker, J., Perkins, A. S., Robertson, E. J. and Efstratiadis, A.** (1993). Mice carrying null mutations of the genes encoding insulin-like growth factor I (Igf-1) and type 1 IGF receptor (Igf1r). *Cell* **75**, 59-72.

**Logan, M., Martin, J. F., Nagy, A., Lobe, C., Olson, E. N. and Tabin, C. J.** (2002). Expression of Cre Recombinase in the developing mouse limb bud driven by a Prxl enhancer. *Genesis* **33**, 77-80.

**Long, F. and Ornitz, D. M.** (2013). Development of the endochondral skeleton. *Cold Spring Harb. Perspect. Biol.* **5**, a008334.

**Long, F., Zhang, X. M., Karp, S., Yang, Y. and McMahon, A. P.** (2001). Genetic manipulation of hedgehog signaling in the endochondral skeleton reveals a direct role in the regulation of chondrocyte proliferation. *Development* **128**, 5099-5108.

**Long, F., Chung, U.-i., Ohba, S., McMahon, J., Kronenberg, H. M. and McMahon, A. P.** (2004). Ihh signaling is directly required for the osteoblast lineage in the endochondral skeleton. *Development* **131**, 1309-1318.

**Long, F., Joeng, K.-S., Xuan, S., Efstratiadis, A. and McMahon, A. P.** (2006). Independent regulation of skeletal growth by Ihh and IGF signaling. *Dev. Biol.* **298**, 327-333.

**Lupu, F., Terwilliger, J. D., Lee, K., Segre, G. V. and Efstratiadis, A.** (2001). Roles of growth hormone and insulin-like growth factor 1 in mouse postnatal growth. *Dev. Biol.* **229**, 141-162.

**Maes, C., Kobayashi, T., Selig, M. K., Torrekens, S., Roth, S. I., Mackem, S., Carmeliet, G. and Kronenberg, H. M.** (2010). Osteoblast precursors, but not mature osteoblasts, move into developing and fractured bones along with invading blood vessels. *Dev. Cell* **19**, 329-344.

**McLeod, M. J.** (1980). Differential staining of cartilage and bone in whole mouse fetuses by alcian blue and alizarin red S. *Teratology* **22**, 299-301.

**Murakami, M., Ichisaka, T., Maeda, M., Oshiro, N., Hara, K., Edenhofer, F., Kiyama, H., Yonezawa, K. and Yamanaka, S.** (2004). mTOR is essential for growth and proliferation in early mouse embryos and embryonic stem cells. *Mol. Cell. Biol.* **24**, 6710-6718.

**Oldham, S. and Hafen, E.** (2003). Insulin/IGF and target of rapamycin signaling: a TOR de force in growth control. *Trends Cell Biol.* **13**, 79-85.

**Polak, P., Cybulski, N., Feige, J. N., Auwerx, J., Rüegg, M. A. and Hall, M. N.** (2008). Adipose-specific knockout of raptor results in lean mice with enhanced mitochondrial respiration. *Cell Metab.* **8**, 399-410.

**Risson, V., Mazelin, L., Roceri, M., Sanchez, H., Moncollin, V., Corneloup, C., Richard-Bulteau, H., Vignaud, A., Baas, D., Defour, A. et al.** (2009). Muscle inactivation of mTOR causes metabolic and dystrophin defects leading to severe myopathy. *J. Cell Biol.* **187**, 859-874.

**Sarbassov, D. D., Ali, S. M., Kim, D.-H., Guertin, D. A., Latek, R. R., Erdjument-Bromage, H., Tempst, P. and Sabatini, D. M.** (2004). Rictor, a novel binding partner of mTOR, defines a rapamycin-insensitive and raptor-independent pathway that regulates the cytoskeleton. *Curr. Biol.* **14**, 1296-1302.

**Sengupta, S., Peterson, T. R., Laplante, M., Oh, S. and Sabatini, D. M.** (2010a). mTORC1 controls fasting-induced ketogenesis and its modulation by ageing. *Nature* **468**, 1100-1104.

**Sengupta, S., Peterson, T. R. and Sabatini, D. M.** (2010b). Regulation of the mTOR complex 1 pathway by nutrients, growth factors, and stress. *Mol. Cell* **40**, 310-322.

**Thoreen, C. C., Kang, S. A., Chang, J. W., Liu, Q., Zhang, J., Gao, Y., Reichling, L. J., Sim, T., Sabatini, D. M. and Gray, N. S.** (2009). An ATP-competitive mammalian target of rapamycin inhibitor reveals rapamycin-resistant functions of mTORC1. *J. Biol. Chem.* **284**, 8023-8032.

**Thoreen, C. C., Chantranupong, L., Keys, H. R., Wang, T., Gray, N. S. and Sabatini, D. M.** (2012). A unifying model for mTORC1-mediated regulation of mRNA translation. *Nature* **485**, 109-113.

**Wang, E., Wang, J., Chin, E., Zhou, J. and Bondy, C. A.** (1995). Cellular patterns of insulin-like growth factor system gene expression in murine chondrogenesis and osteogenesis. *Endocrinology* **136**, 2741-2751.

**Wang, J., Zhou, J. and Bondy, C. A.** (1999). Igf1 promotes longitudinal bone growth by insulin-like actions augmenting chondrocyte hypertrophy. *FASEB J.* **13**, 1985-1990.

**Yilmaz, O. H., Katajisto, P., Lamming, D. W., Gultekin, Y., Bauer-Rowe, K. E., Sengupta, S., Birsoy, K., Dursun, A., Yilmaz, V. O., Selig, M. et al.** (2012). mTORC1 in the Paneth cell niche couples intestinal stem-cell function to calorie intake. *Nature* **486**, 490-495.